SCIENCE CHINA
Information Sciences

• RESEARCH PAPER •

December 2023, Vol. 66 222208:1–222208:16
https://doi.org/10.1007/s11432-022-3738-3

Higher-order temporal interactions promote the cooperation in the multiplayer snowdrift game

Yan XU[1], Juan WANG[2*], Chengyi XIA[3*] & Zhen WANG[4*]

[1]*School of Computer Science and Engineering, Tianjin University of Technology, Tianjin* 300384*, China;*
[2]*School of Electrical Engineering and Automation, Tianjin University of Technology, Tianjin* 300384*, China;*
[3]*School of Artificial Intelligence, Tiangong University, Tianjin* 300387*, China;*
[4]*School of Cyberspace and Center for OPTical IMagery Analysis and Learning (OPTIMAL), Northwestern Polytechnical University, Xi'an* 710072*, China*

Received 17 December 2022/Revised 2 March 2023/Accepted 21 March 2023/Published online 27 November 2023

Abstract To explore evolutionary dynamics of collective behaviors within the interconnected population, previous studies usually map non-pairwise interactions to higher-order static networks. However, from human communications to chemical reactions and biological systems, interactions often change over time, which cannot be simply described by higher-order static networks. In this study, we introduce time effects into higher-order networks and correspondingly investigate the evolutionary dynamics of multiplayer snowdrift games on higher-order temporal networks. Specifically, extensive simulations from four empirical datasets reveal that (1) the temporal effect of higher-order networks can facilitate the evolution of cooperation; (2) the higher-order topology can enhance the emergence of cooperation within a certain range of parameters; (3) the contribution of temporal burstiness and participants burstiness to cooperation is reversed. Furthermore, we theoretically demonstrate that the higher-order structure will suppress the propagation of defection in temporal networks. Our findings offer a new avenue for studying the evolution of altruistic behaviors in realistic complex networks.

Keywords collective behaviors, non-pairwise interactions, multiplayer snowdrift games, temporal networks, higher-order complex networks

Citation Xu Y, Wang J, Xia C Y, et al. Higher-order temporal interactions promote the cooperation in the multiplayer snowdrift game. Sci China Inf Sci, 2023, 66(12): 222208, https://doi.org/10.1007/s11432-022-3738-3

1 Introduction

In addition to dyadic interactions between individuals [1–3], interactions in the real world often occur in groups of more than two elements [4, 5]. For example, multiple scholars jointly complete a scientific research, and wolves collaborate to round up prey. Therefore, it is more relevant to explore the evolution of cooperation in group interactions [6,7]. However, most early studies on the evolution of group cooperation are based on well-mixed populations or traditional networks linked by interacting pairs of nodes [8–14], which do not provide a unique procedure for defining a group [15, 16], and thus an alternative modeling framework is needed to provide an improved description of reality. As a solution, higher-order networks are introduced in evolutionary games that are played in groups. The unique character of higher-order networks is that, apart from traditional networks, they consider simultaneous interactions among multiple nodes [4, 17, 18], allowing them to naturally describe multi-body interactions in the real world.

In recent years, as many scholars have intensively studied higher-order networks, milestone progress has been made in the evolutionary dynamics based on non-dyadic interactions [19]. For instance, Alvarez-Rodriguez et al. [15] studied public goods games on hypergraphs and further confirmed the impact of group size on cooperative behaviors by using empirical data. Schlager et al. [20] proposed the adaptive simplicial snowdrift game, which demonstrated that the stability of the equilibrium points remains unchanged even under higher-order structural frameworks. And moral behavior has also already been studied on higher-order networks [21, 22]. Besides evolutionary dynamics [23], new collective behaviors have also been

* Corresponding author (email: juanwang75@163.com, cyxia@tiangong.edu.cn, zhenwang0@gmail.com)

observed in the field of spreading dynamics [24,25], synchronization phenomena [26,27], and consensus [28, 29] when they are extended beyond pairwise interactions. It should be noted that these important insights regarding the evolution of cooperation on higher-order networks are generally based on a key premise: higher-order interactions (interaction networks) are static.

However, in the real world, time is an important dimension to depict various (pairwise/higher-order) interacting activities, since interactions between individuals will form, strengthen, weaken, or disappear with time. For example, a scholar will collaborate with different individuals at different times to write several distinct papers. Activities such as voice communications, group discussions, and working sessions are also maintained for only a limited period of time. It has been demonstrated that the temporality of interaction activation can significantly influence a variety of dynamical processes, from epidemic spreading [30,31] to event detection [32] and even evolutionary cooperation dynamics [33–36]. Naturally, we consider that temporality will have a far-reaching impact on social systems, over which the relevant dynamic rules are closely related to interactions changing over time. Existing studies usually model higher-order interactions as static networks, which limits the application effectiveness and reliability of the research results in real systems. To solve this problem, we hope to investigate the evolution of cooperation on higher-order temporal networks, driving the expansion of higher-order networks in temporal dimension.

Therefore, we introduce the temporal dimension into higher-order networks and fully consider the chronological sequence of interactions, in order to accurately portray the real systems. On this basis, the evolutionary dynamics of multiplayer snowdrift games is studied. Specifically, (1) we investigate the evolution of cooperation on higher-order temporal networks constructed from empirical datasets, and it is surprising to discover that the temporal effect of higher-order networks can enhance cooperation. (2) We explore the effect of higher-order structures on the emergence of cooperation in time-varying networks, and draw a conclusion that higher-order topology can favor cooperation under some special parameter settings. (3) In many real social systems, interactions are often intermittent and aggregated, indicating that interaction patterns have a bursty character. Thus, we further investigate the impact of bursty behavior on cooperation from the perspective of time and participants. Interestingly, we find that the contribution of temporal and participants burstiness to cooperation is opposite. (4) Finally, we theoretically demonstrate that the higher-order structure will hinder the spread of defection in temporal networks. Our study reveals the significance of temporal information for the evolution of cooperation within the human population.

The remainder of this paper is organized as follows. In Section 2, we present the multiplayer snowdrift game model and higher-order temporal network used in this work. Section 3 provides the numerical results from the simulation. We give the theoretical analysis in Section 4. Section 5 concludes the whole paper and discusses the potential work.

2 Model

2.1 Multiplayer snowdrift game

The multiplayer snowdrift game [37] represents the social dilemma of conflicts between individual and collective interests (i.e., maximizing personal benefits will not maximize group benefits). In this game, each player can choose to shovel the snowdrift (cooperator) or not (defector). The cost c of shoveling the snowdrift is shared equally among the cooperators. Each player, including the defector, will receive an equal benefit $b > c$ if the task is completed. The multiplayer snowdrift game reveals the nature of the social dilemma: contributions may be asymmetric (unbalanced) given equal payoffs. That is to say, there is no relationship between the contribution of players and the distribution of benefits.

The payoffs of cooperators and defectors within the group of K players are calculated as follows:

$$\begin{aligned} \bar{\Pi}_{\mathrm{C}}(n_{\mathrm{c}}) &= b - \frac{c}{n_{\mathrm{c}}}, \quad \text{for } n_{\mathrm{c}} \in [1, K], \\ \bar{\Pi}_{\mathrm{D}}(n_{\mathrm{c}}) &= \begin{cases} 0, & \text{for } n_{\mathrm{c}} = 0, \\ b, & \text{for } n_{\mathrm{c}} \in [1, K-1], \end{cases} \end{aligned} \tag{1}$$

where n_{c} is the number of cooperating players. Let $r = c/b$ represent the cost-to-benefit ratio [37], and

the payoffs can be further normalized and computed as

$$\begin{aligned} \Pi_{\mathrm{C}}(n_{\mathrm{c}}) &= 1 - \frac{r}{n_{\mathrm{c}}}, \quad \text{for } n_{\mathrm{c}} \in [1, K], \\ \Pi_{\mathrm{D}}(n_{\mathrm{c}}) &= \begin{cases} 0, & \text{for } n_{\mathrm{c}} = 0, \\ 1, & \text{for } n_{\mathrm{c}} \in [1, K-1]. \end{cases} \end{aligned} \tag{2}$$

For $K = 2$, the multiplayer snowdrift game will degenerate into a two-player snowdrift game. It should be noted that multiplayer games with $K > 2$ cannot be simplified into multiple two-player encounters [38].

2.2 Higher-order temporal network

We use several empirical datasets to construct the higher-order temporal network, and the construction process is shown in Figure 1. In the investigated datasets, the interactions are initially stored through time-stamped links, as shown in Figure 1(a). There are two factors to be considered in the constructed higher-order temporal networks: (1) the number of individuals involved in the interactions, i.e., the order of interactions, and (2) the sequence of interactions. For the order of interactions, we do not temporally differentiate the interactions occurring within a small time window Δh; that is, we consider that these interactions occur at the same moment. If n players interact two-by-two within a time window Δh, they constitute an $(n-1)$-order interaction. We use simplicial complexes to represent these interactions of different orders. For example, 1-simplex denotes 1-order interaction (two-body interaction), and 2-simplex indicates 2-order interaction (three-body interaction). The construction process of interactions of different orders is shown in Figure 1(b). For the sequence of interactions, we represent higher-order temporal networks by a sequence of snapshots (separate networks) $G = \{G_1, \ldots, G_W\}$ on the same set of N nodes, as shown in Figure 1(c). This discrete method (snapshot sequences) can not only reflect the sequence of interactions, but also capture effective network structures. A snapshot is a static network which is generated by aggregating interactions (simplices) over consecutive, non-overlapping time windows of Δt. Links in different snapshots are independent. For comparison, we also aggregate all simplices by setting $\Delta t = T$ (T is the time span of all interactions in the dataset) to construct higher-order static networks.

2.3 Game process

To simulate the game on a higher-order time-varying structure $\{G_m\}_{m=1,\ldots,W}$, each individual initially behaves either as a cooperator or as a defector with an equal chance on the first snapshot of the sequence, namely on G_1. At each time step, each node plays the snowdrift game in all groups (simplices) to which it belongs. Thus, at time step t, the cumulated payoff of individual i is the sum of the payoffs it receives from each group, which can be expressed as

$$U_i(t) = \sum_{\tau \in \Omega_i} U_{i,\tau}, \tag{3}$$

where Ω_i denotes the collection of simplices to which individual i belongs, and $U_{i,\tau}$ indicates the payoff of individual i obtained from simplex τ. Afterwards, each individual synchronously updates his/her strategy by replicator dynamics rule [39]. Specifically, each individual i randomly selects one of its neighbors j: if $U_i(t) \geqslant U_j(t)$, the current strategy of individual i remains unchanged; if $U_i(t) < U_j(t)$, then individual i adopts the strategy of individual j at the next step with the probability $\phi(s_i(t+1) \leftarrow s_j(t))$, and the strategy transition probability is written as follows:

$$\phi(s_i(t+1) \leftarrow s_j(t)) = \frac{U_j(t) - U_i(t)}{\max\{k_i, k_j\} D}, \tag{4}$$

where k_i and k_j represent individual i's and individual j's generalized degree, respectively, i.e., the number of times they participate in the game, respectively. D is the possible maximum payoff difference between two individuals, and its value depends on the type of game. Here, for MESG, $D = 1$.

The above process denotes a time step, and the same procedure is repeated for g times. Then, we change the network structure to the next snapshot and continue running the game, as shown in Figure 2.

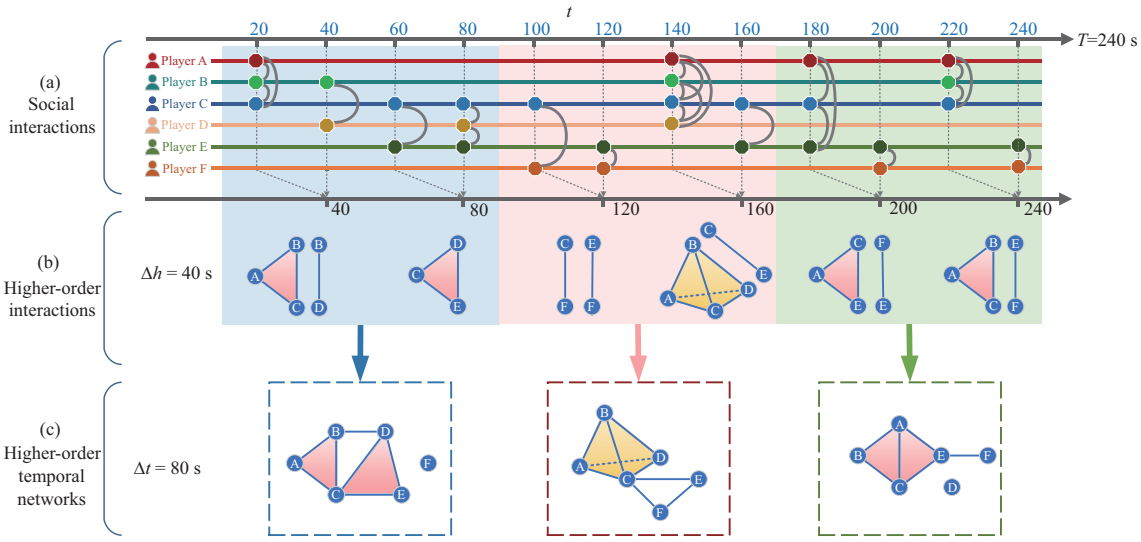

Figure 1 (Color online) Construction of higher-order temporal networks. Here, we show a method for generating higher-order temporal networks using empirical datasets. (a) The sequence of contacts among six players A–F depicted by different colored solid circles. Along the entire time from $t = 0$ to $t = 240$ s, each player corresponds to a horizontal line. During the time interval $(t - \tau, t]$, if two players interact with each other, the corresponding circles will be marked on their respective horizontal lines and connected by a curved line at time t. Here, $\tau = 20$ s. (b) The timestamped simplices constructed from the contact sequence shown in (a) rely on the length of time window Δh. In practice, if in the same window Δh, there are $n(n+1)/2$ edges between a group of n nodes in (a) such that they form a complete graph, we regard these $n(n+1)/2$ edges as an $(n-1)$-simplex. We do not consider interactions that span a long time dimension as higher-order interactions. Thus, the value of Δh is small. Here, $\Delta h = 40$ s. (c) The higher-order temporal networks created from aggregating the simplices shown in (b) into snapshots depend on the length of time windows Δt. Here, $\Delta t = 80$ s. Moreover, when $\Delta t = T$, the entire sequence of snapshots degenerates into a snapshot containing all simplices, i.e., a higher-order static network. The number of snapshots is $\lceil T/\Delta t \rceil$ provided $\Delta t < T$. Generally, we retain only one for simplices that recur in the same Δt; namely, we do not consider the occurrence number of simplices and construct unweighted networks. When constructing weighted networks, each simplex is assigned a weight, and the weight is the occurrence number of the simplex.

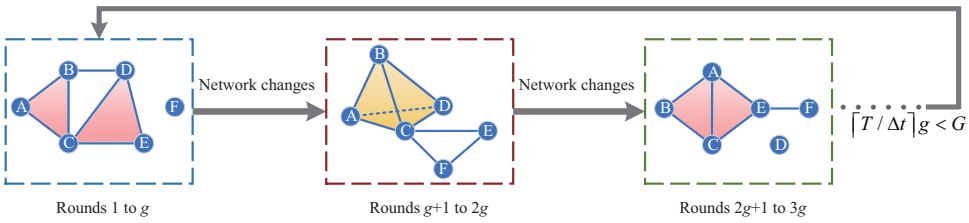

Figure 2 (Color online) Game process on higher-order temporal networks. Here, we show the evolution of the game on some snapshots of higher-order temporal networks. Take the higher-order temporal network corresponding to $\Delta h = 40$ s and $\Delta t = 80$ s in Figure 1(c) as an example. After performing g rounds of evolution in each snapshot, we move to the next one. In all snapshots, we totally run the game for G rounds. If $\lceil T/\Delta t \rceil g < G$, the snapshots are reused according to their sequence.

In all snapshots, the game is performed for a total of G rounds. Note that if $\lceil T/\Delta t \rceil g < G$, i.e., the number of snapshots is insufficient, the sequence of snapshots is reused from the beginning. To obtain the cooperation level at a steady state, we calculate the fraction of cooperators in the system after a long enough evolution time ($G = 10^6$–10^8). Finally, we measure the average frequency of cooperation (f_c) over another 2000 steps. Numerical simulation results are obtained by averaging over 50 independent realizations with random initial conditions. Note that, unlike previous studies [33–35], the time-varying nature of the networks is not related to the dynamics of the game, which allows us to independently assess how temporality affects the game dynamics.

3 Results

3.1 Datasets

We construct higher-order temporal networks to describe real-world interactions by using the publicly available SocioPatterns dataset [40], and then conduct large quantities of experiments. SocioPatterns has

Table 1 Statistics of the datasets. The four datasets we select represent interactions between: participants of an SFHH conference over a period of 2 days on June 4–5, 2009 (SFHH conference), students in 5 classes at a high school in Marseilles, France over 4 days in Dec. 2011 (School 2011), patients, medical doctors, nurses and administrative staffs in a hospital ward in Lyon, France over about 5 days in Dec. 2010 (Hospital 2010), staffs at an office building in France from Jun. 24 to Jul. 5, 2013 (Office 2013). Contacts are defined as individual triples (t, i, j) in the data, which means that node i interacts with j during the time interval $(t, t + 20]$ s. Events (simplices) are k-interactions (k-simplices) among $k + 1$ individuals; namely, these individuals interact two-by-two within the time window Δh. We count the number of events at $\Delta h = 20$ s. The number of snapshots is computed according to the entire time window T over which the data were collected, and the interval Δt is utilized to aggregate the simplices into snapshots.

	SFHH conference	School 2011	Hospital 2010	Office 2013
Number of nodes	403	126	75	92
Number of contacts	70261	28561	32424	9827
Number of events (simplices)	54306	26384	27835	9645
Number of snapshots	$\lceil 114320/\Delta t \rceil$	$\lceil 272350/\Delta t \rceil$	$\lceil 347520/\Delta t \rceil$	$\lceil 987640/\Delta t \rceil$
Recording period (days)	2	4	5	12
Time resolution (s)	20	20	20	20

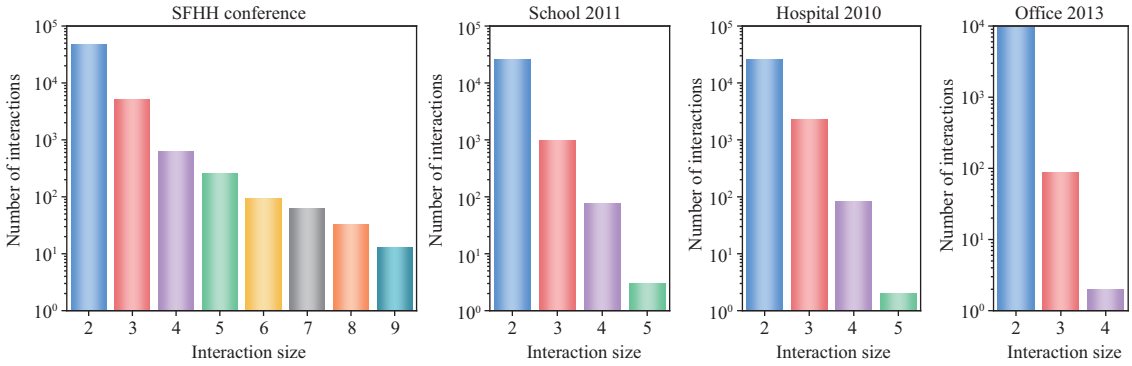

Figure 3 (Color online) Statistics of higher-order interactions. We report the number of interactions for each different size in the four datasets: SFHH conference, School 2011, Hospital 2010, and Office 2013. It is observed that interactions involving more people are fewer.

collected face-to-face interactions of individuals under many realistic settings and recorded them with a time resolution of 20 s. We select four datasets representing different social contexts from SocioPatterns: (a) participants at a scientific conference in Nice, France (SFHH conference) [41], (b) students at a high school in Marseilles, France (School 2011) [42], (c) patients and doctors in a hospital in Lyon, France (Hospital 2010) [43], and (d) staffs at an office building in France (Office 2013) [44]. The statistics of these four datasets is shown in Table 1.

Figure 3 presents the statistics of higher-order interactions for the four datasets. It should be pointed out that, according to [21, 45, 46], we cannot consider interactions that span a long time dimension as higher-order interactions. Therefore, the value of Δh is set to be 20 s in our experiment. Based on this, we count the occurrence number of interactions for different sizes in four datasets. From Figure 3, it can be seen that in four datasets, interactions involving more people are fewer. Moreover, the group sizes are limited to 9, 5, 5, and 4 in the conference, school, hospital, and workplace settings, respectively.

To explore the factors affecting the evolution of cooperation on higher-order temporal networks, we focus on the following scientific questions (SQ):

- SQ1: How does the temporal nature of higher-order networks affect cooperation?
- SQ2: How does the higher-order topology influence cooperation on temporal networks?
- SQ3: How do the burstiness in time and participants impact cooperation?

3.2 Temporal effect of higher-order networks on the evolution of cooperation (SQ1)

Figure 4 illustrates the cooperation rate f_c changing with the cost-to-benefit ratio r and the number of games g on each snapshot under different values of aggregation time window Δt for higher-order temporal networks created from four empirical datasets: (a) SFHH conference, (b) School 2011, (c) Hospital 2010, and (d) Office 2013. As can be seen from Figure 4, f_c declines with the increment of r, which is consistent with previous studies. Furthermore, we also observe a certain range of g (when g is large) over which f_c in higher-order temporal networks is larger than that in their static counterparts, for almost all values of r. The reason is that when g is small (i.e., fewer games performed in each snapshot), the cooperation

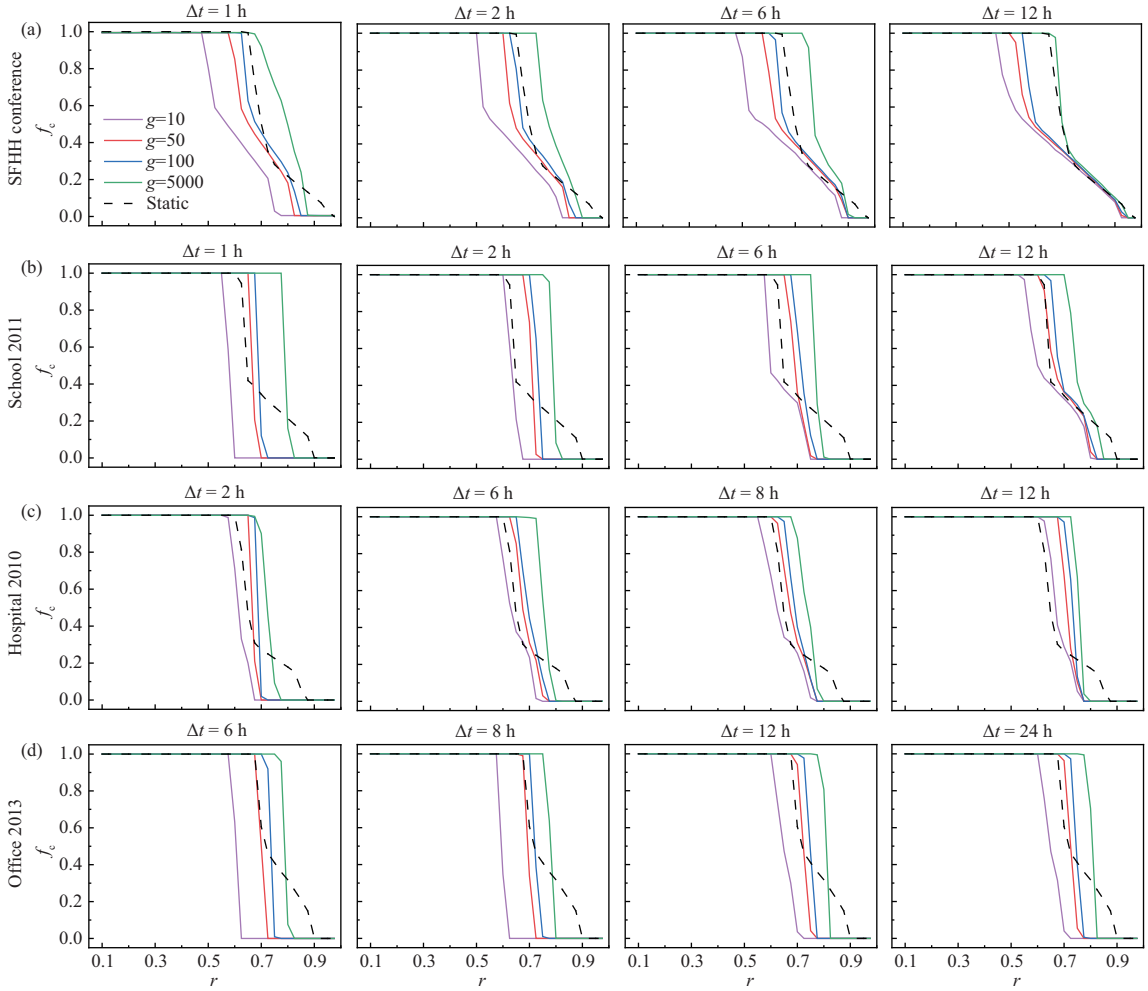

Figure 4 (Color online) Temporal effect of higher-order social structures on the emergence of group cooperation. For four empirical datasets, (a) SFHH conference, (b) School 2011, (c) Hospital 2010, and (d) Office 2013, we present the cooperation level (f_c) at the equilibrium as a function of the cost-to-benefit ratio r on higher-order static (black dashed lines) and temporal (colored solid lines) networks with different values of the aggregation interval Δt. For different datasets, we choose intervals depending on their time span [36]. From left to right, the values of Δt are set to be 1, 2, 6, 12 h in (a) and (b), 2, 6, 8, 12 h in (c), and 6, 8, 12, 24 h in (d), respectively. The frequency of cooperation is obtained by averaging over another 2000 time steps after $G = 10^6$–10^8 time steps are discarded on each higher-order temporal network. It can be shown that the temporal effect of higher-order networks can promote cooperation.

pattern has no chance to stabilize before being destroyed by the next change in network structure, which is detrimental to the evolution of cooperation. Surprisingly, the temporal effect of higher-order networks can still foster cooperation even for small Δt when compared with higher-order static networks.

It is worth mentioning that in higher-order temporal networks, f_c rises as the number of games g at each snapshot increases. By the further expansion, we can obtain the following. (1) The faster the frequency of games (communication) at the same time, i.e., the more the number of games (the greater the g), the greater the fraction of cooperators. From the perspective of social development, with the progress of transportation and communication technology (the frequency of communication increases), the number of exchanges at the same time increases, which is conducive to cooperation. As a result, the pace of social development accelerates. (2) Under the same frequency of exchange, the longer the evolution time (the larger the g), the greater the fraction of cooperators. From the perspective of network development, the change of the network pattern is equivalent to snapshot switching. The slower the snapshot switches, the greater the number of games g in each snapshot, the more conducive to cooperation and network development.

Figure 5 reports the frequency of cooperation $f_c(t)$ as a function of time (game round) under different values of r. It is interesting to observe that regardless of the value of g, the cooperation rate converges quickly and monotonically toward equilibrium with time. The cooperation frequency f_c increases when

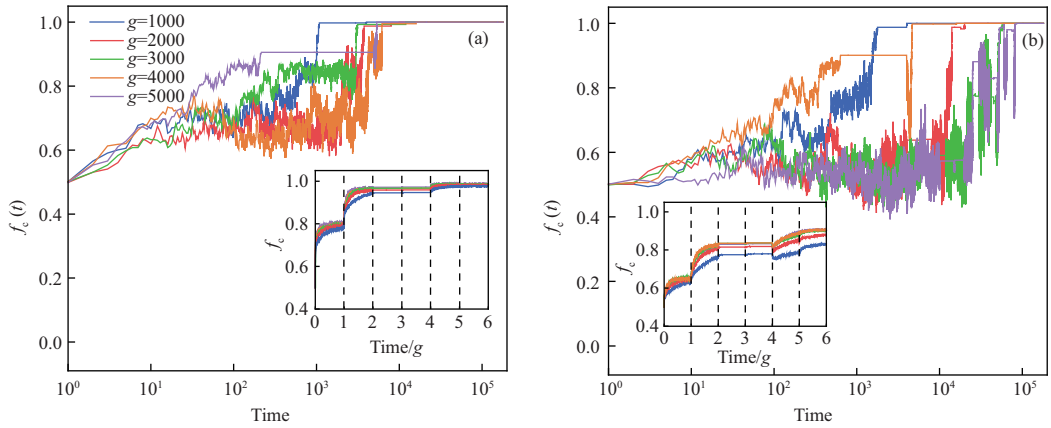

Figure 5 (Color online) Dynamics of the cooperation rate ($f_c(t)$) under different cost-to-benefit ratios r as a function of time. Each curve is obtained over one realization. The horizontal axis in the inset denotes the normalized time scale for different g, i.e., the number of snapshots that completed the evolution. Each curve in the inset is averaged over 500 independent realizations. It is observed that regardless of the value of g, f_c increases when the snapshot switches (denoted by the dashed lines). This means that the evolution of snapshots favors cooperation. Here $r = 0.2$ (a) and $r = 0.5$ (b) with $\Delta t = 6$ h for the SFHH conference dataset.

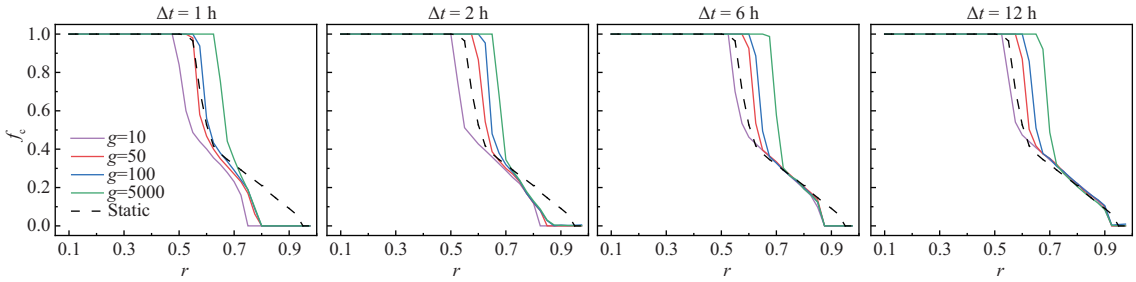

Figure 6 (Color online) Evolution of cooperation on weighted higher-order temporal networks. We report the frequency of cooperation (f_c) at the stationary state as a function of the cost-to-benefit ratio r on weighted higher-order static (black dashed lines) and temporal (colored solid lines) networks with different Δt for the SFHH conference dataset. We observe that the conclusion shown in Figure 4 still holds when we consider weighted networks. Other parameters are the same as those in Figure 4, and results shown here are also applicable for the other three datasets.

the snapshot switches (denoted by the vertical dashed lines in the inset). This suggests that the evolution of network snapshots favors the increase of f_c.

The higher-order temporal networks constructed above are unweighted networks and cannot capture the strength or number of interactions. Therefore, we create weighted networks using the same datasets. Specifically, each simplex is assigned a weight, and the weight is the occurrence number of the simplex in the same Δt. Figure 6 illustrates how the average proportion of cooperators depends on the parameters r and g and on aggregation time window Δt in weighted higher-order temporal networks. It can be seen from Figure 6 that in weighted networks, temporal networks can still foster cooperation compared with their static counterparts. This confirms that our conclusions are robust for weighted networks.

3.3 Impact of higher-order structures on the emergence of cooperation (SQ2)

To explore the effect of higher-order structures on cooperative evolution, we create pairwise temporal networks according to [36]. This method first generates links based on contact sequences and then aggregates these links into snapshots. Figure 7 displays f_c varying with r under different values of Δt and g. From Figure 7, it can be seen that f_c decreases with the increase of r in both pairwise and higher-order temporal networks. This is because, in pairwise and higher-order temporal networks, the increment of r will increase the payoff difference between cooperators and defectors, which makes cooperators choose the defection strategy and thus leads to the decrease of the cooperation level.

When r is small ($r < 0.6$ approximately), the cooperation rates of pairwise and higher-order temporal networks are equal. As r increases ($0.6 < r < 0.7$ approximately), f_c in the higher-order temporal network is larger compared with its pairwise counterpart. This is because, at this moment, the global cooperation level is high, i.e., the number of cooperators in the network is much higher than that of defectors. Since

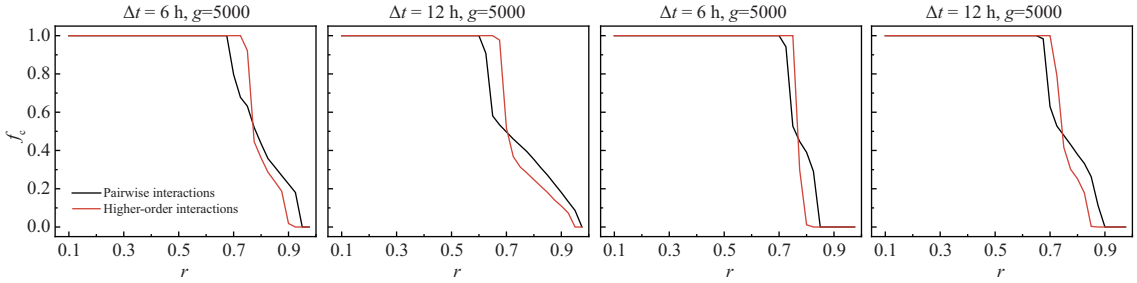

Figure 7 (Color online) Effect of higher-order structures on the evolution of cooperation. We plot the equilibrium cooperation level (f_c) as a function of the cost-to-benefit ratios r on pairwise (gray lines) and higher-order (red lines) temporal networks for the SFHH conference dataset (the left two) and the School 2011 dataset (the right two). We find that the higher-order topology can enhance cooperation within a certain range of parameters. Other parameters are the same as those in Figure 4, and results shown here are also applicable for the other two datasets.

there are more people involved in each game in higher-order structures, the cost of shoveling will be shared among more cooperators. Thus, the payoff difference between cooperators and defectors in higher-order temporal networks is smaller than that in pairwise temporal networks. This indicates that to some extent, higher-order structures can foster cooperation. With the further increase of r ($r > 0.7$ approximately), f_c in the higher-order temporal network decreases faster than that in its pairwise counterpart. This is because, as r increases, f_c in higher-order and pairwise temporal networks decreases and the number of defectors in the network increases. Since there are more people involved within each game in higher-order structures, it is easier to find a cooperator to perform the task and defectors have a higher probability of payoff 1 in higher-order temporal networks. This leads to a greater payoff difference between cooperators and defectors in higher-order temporal networks compared with their pairwise counterparts. Therefore, f_c decreases faster in higher-order temporal networks than in their pairwise counterparts to the extent that it is smaller than in pairwise temporal networks. Note that, our results hold true for other strategy update rule that allows players to copy the strategy with a higher average payoff among its neighbors.

3.4 Role of burstiness in the evolution of cooperation (SQ3)

We consider that the burstiness of higher-order interactions is mainly reflected in two dimensions: temporal burstiness (interactions are aggregated on certain time periods) and participants burstiness (interactions are concentrated on certain individuals). Next, we explore the role of these two aspects, respectively.

(1) Temporal burstiness. There is increasing evidence that temporal patterns of higher-order human interactions, ranging from communication to work and entertainment patterns, have a bursty character: long periods of inactivity that separate bursts of intense activity [47]. The burstiness is also present in the empirical dataset we study, as shown in Figure 8. This figure depicts the occurrence time of interactions of different sizes in the SFHH conference dataset. It can be observed that the appearance of higher-order interactions is highly aggregated in time; that is, they have temporal burstiness. This temporal correlation in activities has been proven to affect the dynamics on networks, for example, accelerating the spread of disease [48]. This motivates us to explore the effect of temporal burstiness on the evolution of cooperation.

Accordingly, we shuffle each dataset to eliminate the burstiness inherent to human interaction data. We adopt the most random timeline shuffling method $P[\mathcal{L}, \mathcal{E}]$ [49], where we redistribute the events between all timelines at random. By uniformly reshuffling the original timelines of interactions, we obtain the randomized higher-order time-varying networks on which the multiplayer snowdrift games are simulated.

Figure 9 plots the quantitative differences between the cooperation level of the original datasets and their randomized versions, as a function of r and g. As can be seen from Figure 9, the cooperation frequency f_c^{RTI} in reshuffled networks minus f_c^{ORI} over the original datasets is almost positive. This suggests that cooperation is enhanced after randomization (the bursty patterns are destroyed); that is, temporal burstiness impedes cooperation. This is because the temporal burstiness of interactions makes it difficult for cooperating players to form stable clusters in order to benefit from mutual cooperation and thus make up for the losses against defectors [50].

Interestingly, we also observe that the explosion of interactions involving more individuals is always accompanied by that of interactions involving fewer agents; that is, the occurrence time of interactions

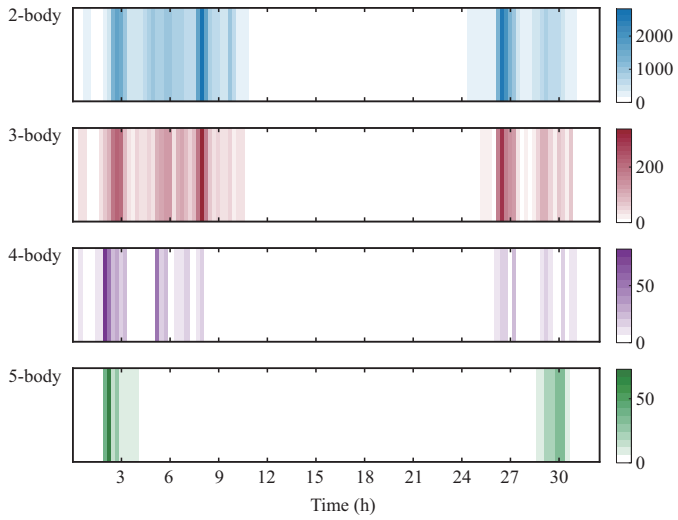

Figure 8 (Color online) Time series of interactions in the SFHH conference dataset. The number of interactions at time t is reported as a function of time. We separate the interactions in accordance with their size: 2-body (blue), 3-body (red), 4-body (purple), and 5-body (green) interactions. We find that higher-order interactions are highly aggregated in time; namely, they have temporal burstiness. Other datasets also present similar time series.

involving fewer individuals always covers that of interactions involving more agents (see Figure 8). This suggests that bursty patterns of interactions are not independent across different orders; i.e., there is a strong dependency among them. This is because higher-order structures always develop from lower-order events. For instance, when A communicates with B, the addition of F increases the interaction size.

To erase the dependencies between temporal bursty patterns, we follow the most random sequence shuffling method $P\left[p_\tau(\Gamma)\right]$ [49], where we shuffle the occurrence time between higher-order interactions with the same size. This method ensures that events of different sizes are independent of each other in the case of time distribution unchanged. After shuffling the interactions in the original datasets, we obtain randomized versions of higher-order time-varying networks and perform the corresponding simulations.

Figure 10 represents the cooperation level $f_{\mathrm{c}}^{\mathrm{RSE}}$ in the randomized graphs minus $f_{\mathrm{c}}^{\mathrm{ORI}}$ in the original datasets varies with r and g. As can be seen from Figure 10, $f_{\mathrm{c}}^{\mathrm{RSE}} - f_{\mathrm{c}}^{\mathrm{ORI}}$ is almost positive, indicating that cooperation is facilitated after randomization (the dependency relationships are destroyed). That is, the dependency relationships among bursty patterns inhibit cooperation.

(2) Participants burstiness. Analyses of the participants of human higher-order interactions in certain realistic scenarios and empirical datasets have revealed a bursty character: higher-order interactions are always concentrated at a small number of individuals. For example, in colleges and universities, those who frequently attend academic conferences are research faculty. To further verify the above conclusion, taking the SFHH conference dataset as an example, we count the number of times each node participates in higher-order interactions, as shown in Figure 11. From Figure 11, it can be seen that higher-order interactions are always concentrated on certain nodes, indicating that higher-order events are burst in terms of participants. Hence, we examine the impact of participants burstiness on the evolution of cooperation.

To this end, we reshuffle the higher-order interactions in the dataset to remove participants burstiness. Here, we use the most random snapshot shuffling method $P\left[t\right]$ [49], where we keep the interaction size unchanged and shuffle the participants of higher-order interactions. This shuffling ensures that nodes in higher-order interactions are completely randomized while keeping the number of interactions of different sizes unaltered. By reshuffling the higher-order interactions in the original dataset, we obtain a randomized version of the higher-order temporal network over which we simulate the games.

Figure 12 shows the cooperation rate $f_{\mathrm{c}}^{\mathrm{ORI}}$ in the original datasets minus $f_{\mathrm{c}}^{\mathrm{RSN}}$ in reshuffled networks as a function of r and g. It can be observed that $f_{\mathrm{c}}^{\mathrm{ORI}} - f_{\mathrm{c}}^{\mathrm{RSN}}$ is almost positive; i.e., the cooperation level in the original datasets is larger than that in the randomized graphs. This suggests that participants burstiness of higher-order interaction can facilitate the cooperation.

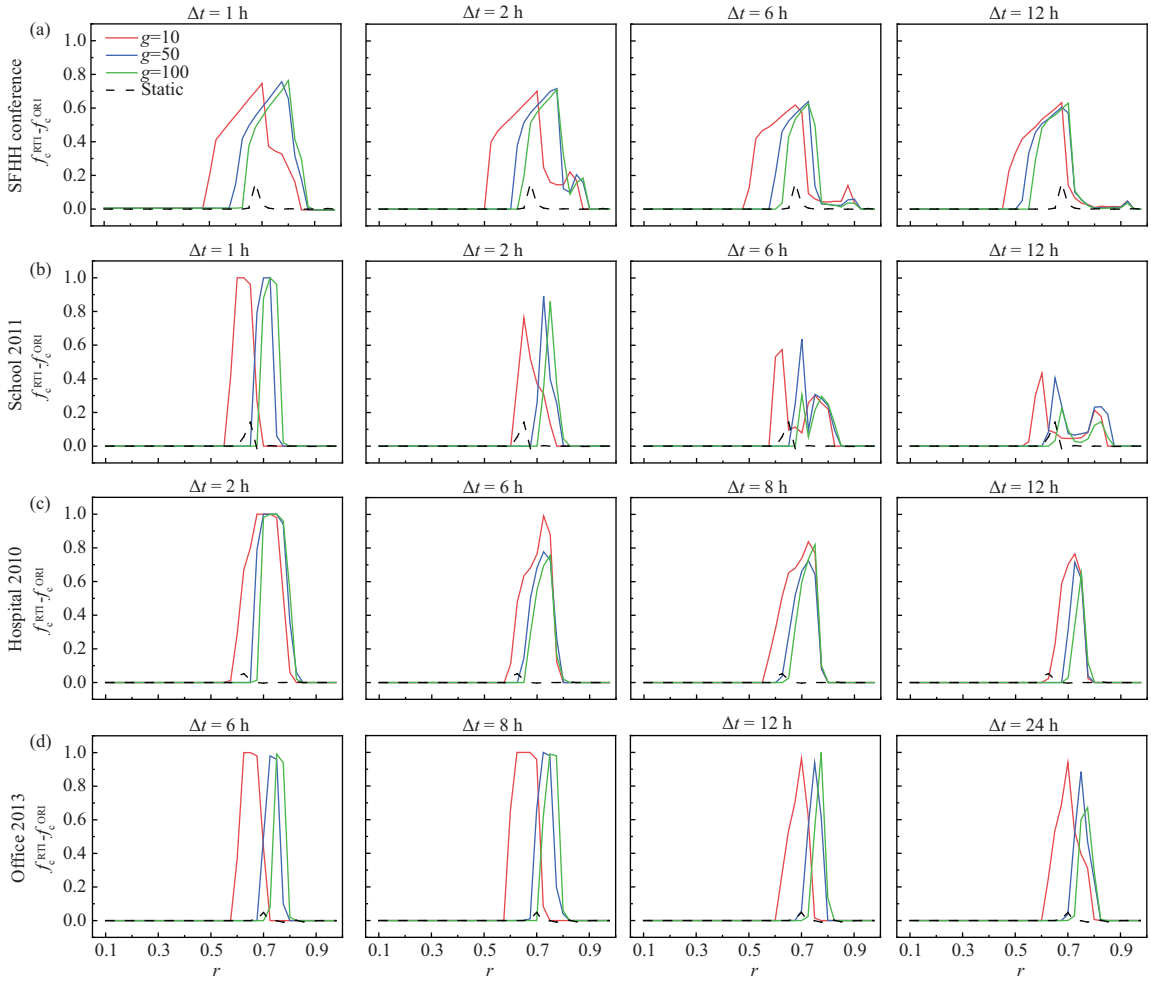

Figure 9 (Color online) Role of temporal burstiness in the evolution of cooperation. For four datasets, (a) SFHH conference, (b) School 2011, (c) Hospital 2010, and (d) Office 2013, we report the difference $f_c^{\mathrm{RTI}} - f_c^{\mathrm{ORI}}$ between the cooperation rate f_c^{RTI} obtained on the reshuffled networks and f_c^{ORI} corresponding to the original datasets, as a function of r and g, at different values of the aggregation interval Δt. It is indicated that cooperation is facilitated after bursty patterns are disrupted; that is, temporal burstiness inhibits cooperation. Other parameters are the same as those in Figure 4.

4 Theoretical analysis

To further investigate the role of higher-order structure in the emergence of cooperation, we theoretically model and analyze the higher-order and pairwise temporal networks, respectively. Specifically, we model higher-order temporal networks by using the simplicial activity-driven (SAD) model [51] and pairwise temporal networks starting from the edge-matched AD (eAD) model [52].

4.1 Higher-order temporal networks (SAD model)

We model higher-order temporal networks using the SAD model. In the SAD model, each vertex i is activated with probability v_i, taken from a probability distribution $F(v)$. Activated node randomly selects $h-1$ nodes and forms an $(h-1)$-simplex. The parameter h denotes the collaboration size, which can either be fixed or a random variable taken from a distribution $p(h)$. After interactions, the node may change its own strategy, which can be expressed by the following processes:

$$\begin{cases} C + D + \cdots \xrightarrow{\beta} D + D + \cdots, \\ C + D + \cdots \xrightarrow{\mu} C + C + \cdots, \end{cases} \tag{5}$$

where C means the cooperator, D denotes the defector, β (μ) indicates the average chance of a cooperator (defector) becoming a defector (cooperator) after interactions.

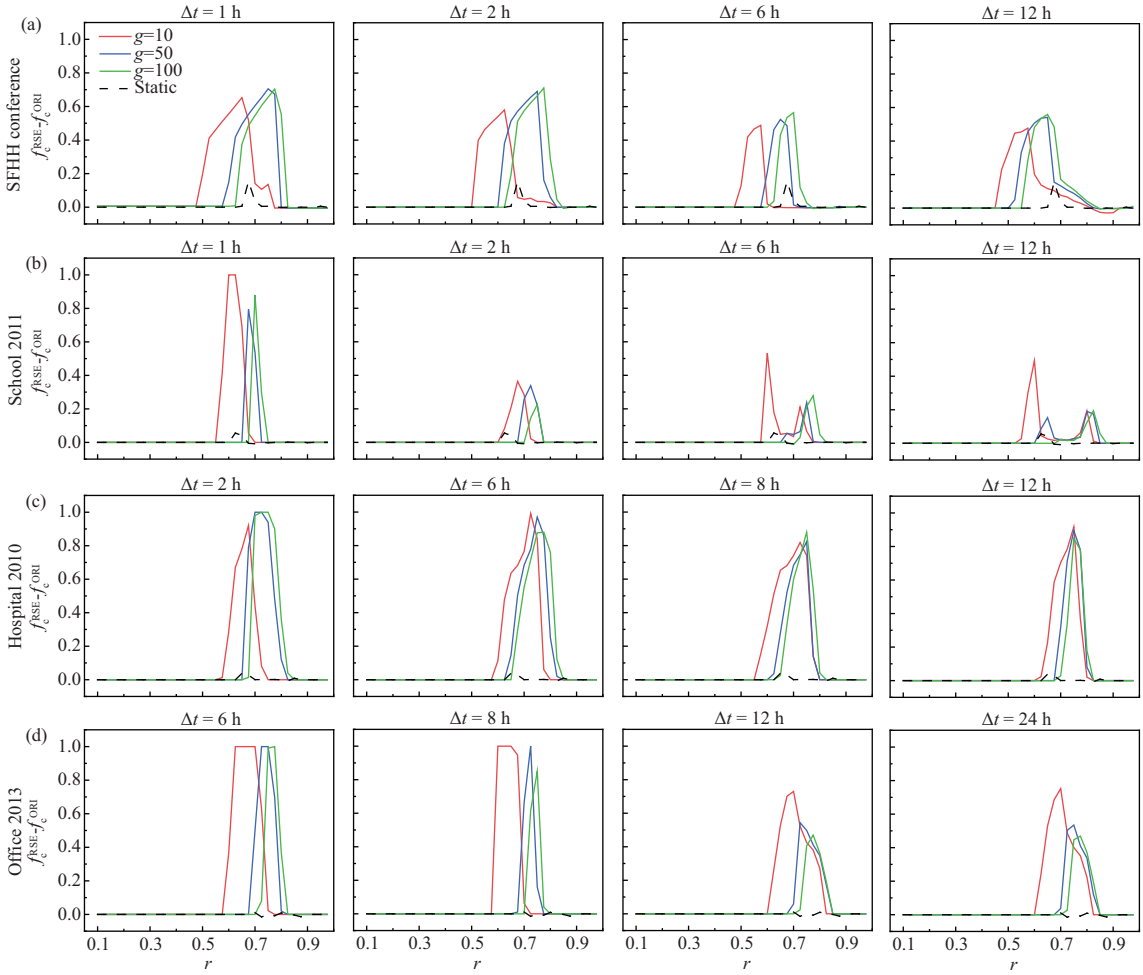

Figure 10 (Color online) Role of dependencies among bursty patterns in the evolution of cooperation. We show the difference $f_c^{\mathrm{RSE}} - f_c^{\mathrm{ORI}}$ between the cooperation rate f_c^{RSE} in the randomized networks and f_c^{ORI} in the original networks, at different values of Δt for (a) SFHH conference, (b) School 2011, (c) Hospital 2010, and (d) Office 2013. We find that cooperation is improved after dependency relationships among bursty patterns are destroyed, suggesting that this relationship suppresses cooperation. Other parameters are the same as those in Figure 4.

Here, we consider the size of the clique generated at each activation in the SAD model is taken from a distribution $p(h)$. Starting from a particular snapshot m, the number of defectors with activity rate υ in the next snapshot, D_υ^{m+1}can be written as

$$D_\upsilon^{m+1} = D_\upsilon^m - \mu D_\upsilon^m + N_{CD} + N_{DC} + N_{CCD}, \tag{6}$$

$$N_{CD} = \int \mathrm{d}h p(h) \left(N_\upsilon - D_\upsilon^m\right) \upsilon(h-1) \int \mathrm{d}\upsilon' D_{\upsilon'}^m \frac{\beta}{N}, \tag{7}$$

$$N_{DC} = \int \mathrm{d}h p(h) \int \mathrm{d}\upsilon' D_{\upsilon'}^m \upsilon'(h-1) \frac{\left(N_\upsilon - D_\upsilon^m\right)}{N} \beta, \tag{8}$$

$$N_{CCD} = \int \mathrm{d}h p(h) \left(N_\upsilon - D_\upsilon^m\right) \frac{\beta}{N} \int \mathrm{d}\upsilon' \left(N_{\upsilon'} - D_{\upsilon'}^m\right) \upsilon'(h-1) \int \mathrm{d}\upsilon'' \frac{D_{\upsilon''}^m}{N} (h-2), \tag{9}$$

where D_υ^m represents the number of defectors with activity υ in snapshot m, μD_υ^m denotes the number of defectors with activity υ that convert to cooperators, N_{CD} means active cooperators with activity υ create an $(h-1)$-simplex that includes defectors with any activity (hence the integration over υ') and adopt defectors' strategy, N_{DC} describes cooperators with activity υ share an $(h-1)$-simplex with active defectors with any activity and copy defectors' strategy, N_{CCD} denotes cooperators with activity υ are chosen by an active cooperator with any activity who creates an $(h-1)$-simplex that also contains defectors with any activity, and imitates defectors' strategy, $(N_{CD} + N_{DC} + N_{CCD})$ captures the number

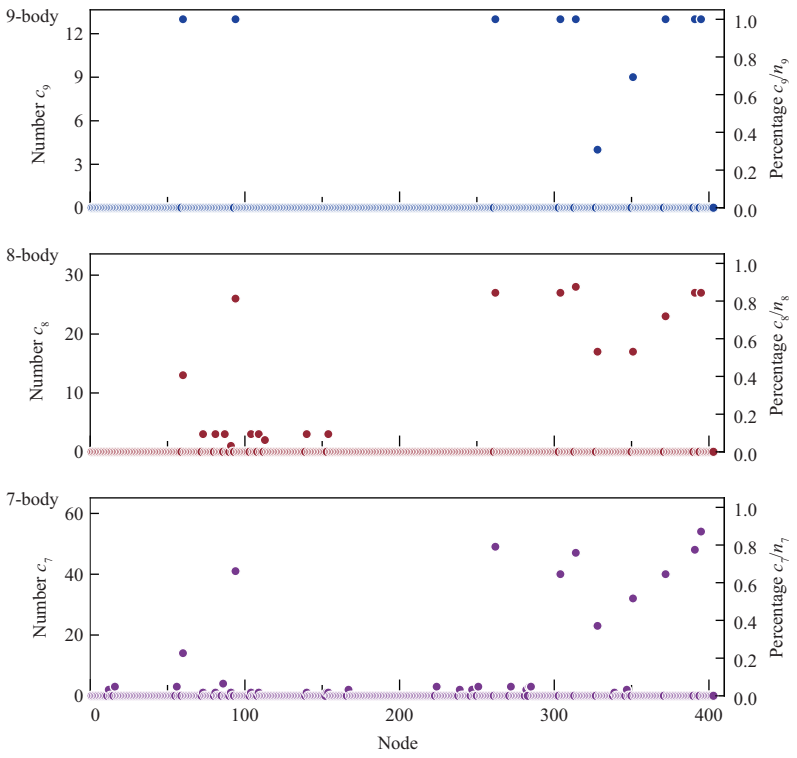

Figure 11 (Color online) Number of times each node participates in higher-order interactions in the SFHH conference dataset. There are 405 participants involved in the conference. The interactions are separated in accordance with their size: 9-body (blue), 8-body (red), and 7-body (purple) interactions. c_i denotes the number of times the corresponding node involved in the i-body interactions. n_i indicates the total number of i-body interactions. We notice that higher-order interactions are always concentrated on certain nodes, indicating that higher-order events are burst in terms of participants.

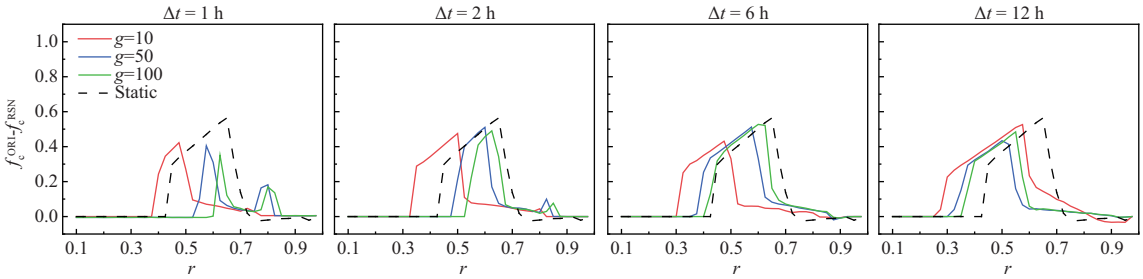

Figure 12 (Color online) Role of participants burstiness in the emergence of cooperation. We depict the difference $f_c^{\mathrm{ORI}} - f_c^{\mathrm{RSN}}$ between the cooperation rate in higher-order temporal networks created from the original and randomized SFHH conference dataset. It is clearly exhibited that $f_c^{\mathrm{ORI}} - f_c^{\mathrm{RSN}}$ is almost positive, indicating that participants burstiness of higher-order interaction can favor cooperation. Other parameters are the same as those in Figure 4.

of cooperators with activity υ that convert to defectors, N_υ means the total number of individuals with activity υ, $N_\upsilon - D_\upsilon^m$ means the number of cooperators with activity υ in snapshot m, $N = \int \mathrm{d}\upsilon N_\upsilon$ is the whole population, $\int \mathrm{d}\upsilon D_\upsilon^m$ denotes the total number of defectors in snapshot m, and we define it as D^m.

By integrating (6) over all values of υ, we can obtain the equation:

$$D^{m+1} = D^m - \mu D^m + \beta\langle h-1\rangle\langle\upsilon\rangle D^m + \beta\langle h-1\rangle G^m + \beta\langle(h-1)(h-2)\rangle\langle\upsilon\rangle D^m, \tag{10}$$

considering that

$$\int \mathrm{d}\upsilon N_{CD} = \int \mathrm{d}\upsilon \int \mathrm{d}h p(h)\left(N_\upsilon - D_\upsilon^m\right)\upsilon(h-1)\int \mathrm{d}\upsilon' D_{\upsilon'}^m \frac{\beta}{N} = \beta\langle h-1\rangle\langle\upsilon\rangle D^m, \tag{11}$$

$$\int \mathrm{d}\upsilon N_{DC} = \int \mathrm{d}\upsilon \int \mathrm{d}h p(h) \int \mathrm{d}\upsilon' D_{\upsilon'}^m \upsilon'(h-1)\frac{\left(N_\upsilon - D_\upsilon^m\right)}{N}\beta = \beta\langle h-1\rangle G^m, \tag{12}$$

and

$$\begin{aligned}\int \mathrm{d}\upsilon N_{CCD} &= \int \mathrm{d}\upsilon \int \mathrm{d}hp(h)\left(N_\upsilon - D_\upsilon^m\right)\frac{\beta}{N}\int \mathrm{d}\upsilon'\left(N_{\upsilon'} - D_{\upsilon'}^m\right)\upsilon'(h-1)\int \mathrm{d}\upsilon''\frac{D_{\upsilon''}^m}{N}(h-2)\\ &= \beta\langle(h-1)(h-2)\rangle\langle\upsilon\rangle D^m,\end{aligned} \tag{13}$$

where $G^m = \int \mathrm{d}\upsilon D_\upsilon^m \upsilon$.

To get a closed equation for G^m, we multiply (6) by υ and integrate over υ, obtaining the equation:

$$G^{m+1} = G^m - \mu G^m + \beta\langle h-1\rangle\left\langle\upsilon^2\right\rangle D^m + \beta\langle h-1\rangle\langle\upsilon\rangle G^m + \beta\langle(h-1)(h-2)\rangle\langle\upsilon\rangle^2 D^m, \tag{14}$$

considering that

$$\int \mathrm{d}\upsilon\upsilon N_{CD} = \int \mathrm{d}\upsilon\upsilon \int \mathrm{d}hp(h)\left(N_\upsilon - D_\upsilon^m\right)\upsilon(h-1)\int \mathrm{d}\upsilon' D_{\upsilon'}^m \frac{\beta}{N} = \beta\langle h-1\rangle\left\langle\upsilon^2\right\rangle D^m, \tag{15}$$

$$\int \mathrm{d}\upsilon\upsilon N_{DC} = \int \mathrm{d}\upsilon\upsilon \int \mathrm{d}hp(h)\int \mathrm{d}\upsilon' D_{\upsilon'}^m \upsilon'(h-1)\frac{\left(N_\upsilon - D_\upsilon^m\right)}{N}\beta = \beta\langle h-1\rangle\langle\upsilon\rangle G^m, \tag{16}$$

and

$$\begin{aligned}\int \mathrm{d}\upsilon\upsilon N_{CCD} &= \int \mathrm{d}\upsilon\upsilon \int \mathrm{d}hp(h)\left(N_\upsilon - D_\upsilon^m\right)\frac{\beta}{N}\int \mathrm{d}\upsilon'\left(N_{\upsilon'} - D_{\upsilon'}^m\right)\upsilon'(h-1)\int \mathrm{d}\upsilon''\frac{D_{\upsilon''}^m}{N}(h-2)\\ &= \beta\langle(h-1)(h-2)\rangle\langle\upsilon\rangle^2 D^m.\end{aligned} \tag{17}$$

In the continuum limit for time m, we obtain the expressions for dynamics of D and G as follows:

$$\begin{cases}\partial_m D = -\mu D + \beta\left\langle(h-1)^2\right\rangle\langle\upsilon\rangle D + \beta\langle h-1\rangle G,\\ \partial_m G = -\mu G + \beta\langle h-1\rangle\left\langle\upsilon^2\right\rangle D + \beta\langle h-1\rangle\langle\upsilon\rangle G + \beta\langle(h-1)(h-2)\rangle\langle\upsilon\rangle^2 D.\end{cases} \tag{18}$$

By linearizing the above system at the origin, we obtain the corresponding Jacobian matrix

$$J = \begin{pmatrix} -\mu + \beta\left\langle(h-1)^2\right\rangle\langle\upsilon\rangle & \beta\langle h-1\rangle \\ \beta(\langle h-1\rangle\left\langle\upsilon^2\right\rangle + \langle(h-1)(h-2)\rangle\langle\upsilon\rangle^2) & -\mu + \beta\langle h-1\rangle\langle\upsilon\rangle \end{pmatrix}, \tag{19}$$

with the eigenvalues

$$\Lambda_{1,2} = \left(\beta\langle h(h-1)\rangle\langle\upsilon\rangle - 2\mu \pm \beta\sqrt{\langle(h-1)(h-2)\rangle\langle(h-1)(h+2)\rangle\langle\upsilon\rangle^2 + 4\langle h-1\rangle^2\left\langle\upsilon^2\right\rangle}\right)/2.$$

When the largest one is positive, defectors will not vanish in the population as a whole. This yields the threshold for instability of the no-defection equilibrium:

$$\frac{\beta}{\mu} > \lambda_{\mathrm{c}}^{\mathrm{SAD}}, \tag{20}$$

$$\lambda_{\mathrm{c}}^{\mathrm{SAD}} = \frac{2}{\langle h(h-1)\rangle\langle\upsilon\rangle + \sqrt{\langle(h-1)(h-2)\rangle\langle(h-1)(h+2)\rangle\langle\upsilon\rangle^2 + 4\langle h-1\rangle^2\left\langle\upsilon^2\right\rangle}}. \tag{21}$$

4.2 Pairwise temporal networks (eAD model)

To compare with the SAD model, we model pairwise temporal networks using the edge-matched AD (eAD) model. In the eAD model, the active node generates $h(h-1)/2$ links that are connected to $h(h-1)/2$ other randomly selected nodes.

Similar to the SAD model, the equation for the evolution of D_υ^m in the eAD model can be written as

$$D_\upsilon^{m+1} = D_\upsilon^m - \mu D_\upsilon^m + N'_{CD} + N'_{DC}, \tag{22}$$

$$N'_{CD} = \int \mathrm{d}hp(h)\left(N_\upsilon - D_\upsilon^m\right)\upsilon\frac{h(h-1)}{2}\int \mathrm{d}\upsilon' D_{\upsilon'}^m\frac{\beta}{N}, \tag{23}$$

Table 2 Values of $\lambda_{\rm c}^{\rm SAD}/\lambda_{\rm c}^{\rm eAD}$ for empirical datasets. We measure $F(v)$ and $p(h)$ at different Δt for each dataset, and calculate $\lambda_{\rm c}^{\rm SAD}/\lambda_{\rm c}^{\rm eAD}$ using (26)

Dataset	1 h	2 h	6 h	12 h
SFHH conference	1.0420	1.0366	1.0310	1.0194
School 2011	1.0135	1.0111	1.0160	1.0171
Hospital 2010	1.0339	1.0262	1.0227	1.0082
Office 2013	1.0024	1.0018	1.0010	1.0002

$$N'_{DC}=\int {\rm d}hp(h)\left(N_v-D_v^m\right)\int {\rm d}v'D_{v'}^m v'\frac{h(h-1)}{2}\frac{\beta}{N}, \tag{24}$$

where D_v^m represents the number of defectors with activity v in snapshot m, μD_v^m denotes the number of defectors with activity v that convert to cooperators, N'_{CD} means active cooperators with activity v interact with defectors with any activity and imitate defectors' strategy, N'_{DC} stands for cooperators with activity v share a link with active defectors with any activity and imitate defectors' strategy, $(N'_{CD}+N'_{DC})$ captures the number of cooperators with activity v that convert to defectors, N_v means the total number of individuals with activity v, $N_v-D_v^m$ denotes the number of cooperators with activity v in snapshot m, $N=\int {\rm d}vN_v$ describes the whole population, $\int {\rm d}vD_v^m$ means the total number of defectors in snapshot m, and we define it as D^m.

Proceeding as before, we can get the threshold condition:

$$\frac{\beta}{\mu}>\lambda_{\rm c}^{\rm eAD},\quad \lambda_{\rm c}^{\rm eAD}=\frac{2}{\langle h(h-1)\rangle(\langle v\rangle+\sqrt{\langle v^2\rangle})}. \tag{25}$$

4.3 Ratio between SAD and eAD thresholds

Using the expressions for $\lambda_{\rm c}^{\rm SAD}$ and $\lambda_{\rm c}^{\rm eAD}$, we can write the ratio between these two quantities:

$$\frac{\lambda_{\rm c}^{\rm SAD}}{\lambda_{\rm c}^{\rm eAD}}=\frac{\langle v\rangle+\sqrt{\langle v^2\rangle}}{\langle v\rangle+\sqrt{\langle v^2\rangle}\sqrt{\psi}}, \tag{26}$$

$$\psi=\frac{4\langle h-1\rangle^2}{\langle h(h-1)\rangle^2}+\frac{\langle (h-1)(h-2)\rangle\langle (h-1)(h+2)\rangle}{\langle h(h-1)\rangle^2}\cdot\frac{\langle v\rangle^2}{\langle v^2\rangle}. \tag{27}$$

If $\lambda_{\rm c}^{\rm SAD}/\lambda_{\rm c}^{\rm eAD}$ is larger than 1, it means that compared with pairwise temporal networks, higher-order temporal networks are less conducive to the existence of defectors.

For the four empirical datasets investigated in this study, we extract node activity $F(v)$ and clique size $p(h)$ distributions for different Δt. Then, we use (26) to calculate the ratio between the defection propagation thresholds for the SAD and eAD models according to these extracted distributions, and the results are presented in Table 2. In Table 2, the ratio is always larger than 1, meaning that the defection propagation threshold is greater in the SAD model than in the eAD model, i.e., the higher-order structure hinders the propagation of defection. That is, the higher-order structure can foster the evolution of cooperation, which is consistent with our previous result.

5 Conclusion and discussion

The higher-order temporal network is a non-pairwise network model with a time dimension, which can more accurately portray the real system. Exploring the evolutionary dynamics on higher-order temporal networks is extremely important for us to understand the correlation between the network structure and dynamics on top of networks, and then to discover the intrinsic motivation for group cooperation.

In this study, we use four empirical datasets to construct higher-order temporal networks on which the evolutionary dynamics of multiplayer snowdrift games are investigated. We find that, compared with higher-order static networks, higher-order temporal networks can favor the evolution of cooperation. By comparing higher-order and pairwise temporal networks, it is found that higher-order structures can improve cooperation within a certain parameter range. We further explore the effect of burstiness on cooperation in terms of both time and participants. Results show that temporal burstiness inhibits the cooperation, while participants burstiness presents the adverse effect. Moreover, we theoretically model higher-order and pairwise temporal networks by using SAD and eAD models, respectively, to further

study the role of higher-order structure in cooperative dynamics on temporal networks. We demonstrate that higher-order structures can hinder the propagation of defection.

Notably, we only consider a single social relationship network. However, in reality, individuals often have multiple identities and participate in multiple relationship networks simultaneously, such as virtual network and real physical contact network and so on [53]. Individuals often behave differently when they are in different relationship networks, and their benefits depend on the corresponding interactions in different networks. Multi-layer higher-order temporal networks can more accurately depict multiple interaction scenarios. Thus, it is meaningful to explore the evolution of group cooperation on multi-layer higher-order temporal networks.

Moreover, the modeling of time window will lead to the discretization of temporal information, which is not consistent with the continuous nature of time. In future work, it is of great significance to find a network modeling method that can reflect the continuous characteristics of interaction time. Overall, our findings advance the study of evolutionary games on more realistic networks and our work opens a new approach for exploring the evolution of cooperative behaviors.

Acknowledgements This work was supported by National Natural Science Foundation of China (Grant Nos. 62025602, 62173247, U1803263), Tianjin Municipal Natural Science Foundation (Grant No. 22JCZDJC00550), and Tianjin University of Technology Postgraduate Research Innovation Project (Grant Nos. YJ2239, YJ2240).

References

1 Du J M, Wu B, Wang L. Aspiration dynamics in structured population acts as if in a well-mixed one. Sci Rep, 2015, 5: 8014
2 Zhou L, Wu B, Du J M, et al. Aspiration dynamics generate robust predictions in heterogeneous populations. Nat Commun, 2021, 12: 3250
3 Su Q, McAvoy A, Mori Y, et al. Evolution of prosocial behaviours in multilayer populations. Nat Hum Behav, 2022, 6: 338–348
4 Battiston F, Cencetti G, Iacopini I, et al. Networks beyond pairwise interactions: Structure and dynamics. Phys Rep, 2020, 874: 1–92
5 Benson A R, Abebe R, Schaub M T, et al. Simplicial closure and higher-order link prediction. Proc Natl Acad Sci USA, 2018, 115: 11221–11230
6 Perc M, Gómez-Gardeñes J, Szolnoki A, et al. Evolutionary dynamics of group interactions on structured populations: a review. J R Soc Interface, 2013, 10: 20120997
7 Li A M, Broom M, Du J M, et al. Evolutionary dynamics of general group interactions in structured populations. Phys Rev E, 2016, 93: 022407
8 Jian Q, Li X P, Wang J, et al. Impact of reputation assortment on tag-mediated altruistic behaviors in the spatial lattice. Appl Math Computation, 2021, 396: 125928
9 Wu B, Traulsen A, Gokhale C S. Dynamic properties of evolutionary multi-player games in finite populations. Games, 2013, 4: 182–199
10 Du J M, Wu B, Altrock P M, et al. Aspiration dynamics of multi-player games in finite populations. J R Soc Interface, 2014, 11: 20140077
11 Su Q, Zhou L, Wang L. Evolutionary multiplayer games on graphs with edge diversity. Plos Comput Biol, 2019, 15: e1006947
12 Govaert A, Cao M. Zero-determinant strategies in repeated multiplayer social dilemmas with discounted payoffs. IEEE Trans Automat Contr, 2020, 66: 4575–4588
13 Wang Z, Jusup M, Guo H, et al. Communicating sentiment and outlook reverses inaction against collective risks. Proc Natl Acad Sci USA, 2020, 117: 17650–17655
14 Guo P L, Wang Y Z, Li H T. Stable degree analysis for strategy profiles of evolutionary networked games. Sci China Inf Sci, 2016, 59: 052204
15 Alvarez-Rodriguez U, Battiston F, de Arruda G F, et al. Evolutionary dynamics of higher-order interactions in social networks. Nat Hum Behav, 2021, 5: 586–595
16 Xu Y, Feng M L, Zhu Y Y, et al. Multi-player snowdrift game on scale-free simplicial complexes. Phys A-Stat Mech Its Appl, 2022, 604: 127698
17 Li D, Song W B, Liu J M. Complex network evolution model based on turing pattern dynamics. IEEE Trans Pattern Anal Mach Intell, 2023, 45: 4229–4244
18 Shi D H, Chen Z, Sun X, et al. Computing cliques and cavities in networks. Commun Phys, 2021, 4: 249
19 Majhi S, Perc M, Ghosh D. Dynamics on higher-order networks: a review. J R Soc Interface, 2022, 19: 20220043
20 Schlager D, Clauß K, Kuehn C. Stability analysis of multiplayer games on adaptive simplicial complexes. Chaos, 2022, 32: 053128
21 Kumar A, Chowdhary S, Capraro V, et al. Evolution of honesty in higher-order social networks. Phys Rev E, 2021, 104: 054308
22 Capraro V, Perc M. Mathematical foundations of moral preferences. J R Soc Interface, 2021, 18: 20200880
23 Civilini A, Anbarci N, Latora V. Evolutionary game model of group choice dilemmas on hypergraphs. Phys Rev Lett, 2021, 127: 268301
24 Iacopini I, Petri G, Barrat A, et al. Simplicial models of social contagion. Nat Commun, 2019, 10: 2485
25 St-Onge G, Sun H, Allard A, et al. Universal nonlinear infection kernel from heterogeneous exposure on higher-order networks. Phys Rev Lett, 2021, 127: 158301
26 Skardal P S, Arenas A. Abrupt desynchronization and extensive multistability in globally coupled oscillator simplexes. Phys Rev Lett, 2019, 122: 248301
27 Ghorbanchian R, Restrepo J G, Torres J J, et al. Higher-order simplicial synchronization of coupled topological signals. Commun Phys, 2021, 4: 120
28 Neuhäuser L, Mellor A, Lambiotte R. Multibody interactions and nonlinear consensus dynamics on networked systems. Phys Rev E, 2020, 101: 032310

29 Sahasrabuddhe R, Neuhäuser L, Lambiotte R. Modelling non-linear consensus dynamics on hypergraphs. J Phys Complex, 2021, 2: 025006
30 Chowdhary S, Kumar A, Cencetti G, et al. Simplicial contagion in temporal higher-order networks. J Phys Complex, 2021, 2: 035019
31 Wang H, Zhang H F, Zhu P C, et al. Interplay of simplicial awareness contagion and epidemic spreading on time-varying multiplex networks. Chaos, 2022, 32: 083110
32 Li X, Zhang X, Huangpeng Q Z, et al. Event detection in temporal social networks using a higher-order network model. Chaos, 2021, 31: 113144
33 Wu B, Zhou D, Fu F, et al. Evolution of cooperation on stochastic dynamical networks. Plos One, 2010, 5: e11187
34 Wu B, Zhou D, Wang L. Evolutionary dynamics on stochastic evolving networks for multiple-strategy games. Phys Rev E, 2011, 84: 046111
35 Du J, Wu Z R. Evolutionary dynamics of cooperation in dynamic networked systems with active striving mechanism. Appl Math Computation, 2022, 430: 127295
36 Li A M, Zhou L, Su Q, et al. Evolution of cooperation on temporal networks. Nat Commun, 2020, 11: 2259
37 Chiong R, Kirley M. Effects of iterated interactions in multiplayer spatial evolutionary games. IEEE Trans Evol Computat, 2012, 16: 537–555
38 Gokhale C S, Traulsen A. Evolutionary games in the multiverse. Proc Natl Acad Sci USA, 2010, 107: 5500–5504
39 Zhang J L, Cao M. Strategy competition dynamics of multi-agent systems in the framework of evolutionary game theory. IEEE Trans Circuits Syst II, 2020, 67: 152–156
40 Kibanov M, Atzmueller M, Scholz C, et al. Temporal evolution of contacts and communities in networks of face-to-face human interactions. Sci China Inf Sci, 2014, 57: 032103
41 Génois M, Barrat A. Can co-location be used as a proxy for face-to-face contacts? EPJ Data Sci, 2018, 7: 11
42 Fournet J, Barrat A. Contact patterns among high school students. Plos One, 2014, 9: e107878
43 Vanhems P, Barrat A, Cattuto C, et al. Estimating potential infection transmission routes in hospital wards using wearable proximity sensors. Plos One, 2013, 8: e73970
44 Génois M, Vestergaard C L, Fournet J, et al. Data on face-to-face contacts in an office building suggest a low-cost vaccination strategy based on community linkers. Net Sci, 2015, 3: 326–347
45 Wang H, Ma C, Chen H S, et al. Full reconstruction of simplicial complexes from binary contagion and Ising data. Nat Commun, 2022, 13: 3043
46 Iacopini I, Petri G, Baronchelli A, et al. Group interactions modulate critical mass dynamics in social convention. Commun Phys, 2022, 5: 64
47 Barabási A L. The origin of bursts and heavy tails in human dynamics. Nature, 2005, 435: 207–211
48 Takaguchi T, Masuda N, Holme P. Bursty communication patterns facilitate spreading in a threshold-based epidemic dynamics. Plos One, 2013, 8: e68629
49 Gauvin L, Génois M, Karsai M, et al. Randomized reference models for temporal networks. SIAM Rev, 2022, 64: 763–830
50 Nowak M A, May R M. Evolutionary games and spatial chaos. Nature, 1992, 359: 826–829
51 Petri G, Barrat A. Simplicial activity driven model. Phys Rev Lett, 2018, 121: 228301
52 Perra N, Gonçalves B, Pastor-Satorras R, et al. Activity driven modeling of time varying networks. Sci Rep, 2012, 2: 469
53 Li X-J, Li C, Li X. The impact of information dissemination on vaccination in multiplex networks. Sci China Inf Sci, 2022, 65: 172202